Protein Expression and Purification 227 (2025) 106638

Contents lists available at ScienceDirect

Protein Expression and Purification

journal homepage: www.elsevier.com/locate/yprep

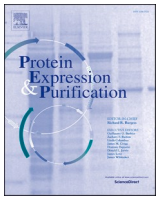

Research Article

# Efficient development of nanobody-based affinity chromatography for AAV8 purification

Guanghui Li [1], Xiaofei Li [1], Min Zhu, Peng Qiao, Weiwei Ji, Yuping Huang, Yicai Zhang, Xuee Li, Yakun Wan [*]

*Shanghai Novamab Biopharmaceuticals Co., Ltd., Shanghai, China*

ARTICLE INFO

*Keywords:*
Nanobody
AAV
Affinity chromatography
Purification
Resin

ABSTRACT

Adeno-associated virus serotype 8 (AAV8) is a highly effective vector for gene therapy. However, its purification remains challenging due to its low natural abundance and stringent purity requirements. This study aimed to develop an affinity chromatography resin utilizing nanobodies (Nbs) to enhance AAV8 purification efficiency. An AAV8-specific Nb library was constructed, leading to the identification of Nb9 as the most promising candidate based on its high binding affinity, stability and yield. Nb9 was expressed in *Pichia pastoris*, resulting in high yield and exceptional purity. Two types of agarose resins, Epoxy activated Bestarose 6B and PabPur SulfoLink Beads 4FF, were employed for Nb9 conjugation. Epoxy activated Bestarose 6B resin exhibited a significantly higher ligand density (9.12 mg/mL). Binding capacity assessments of the LQ01 resin demonstrated optimal performance at pH 7.0, with diminishing efficacy at lower and higher pH levels. Different NaCl concentrations influenced the binding efficiency, providing critical insights for refining purification conditions. Purification trials exhibited high specificity, purity and consistent VP protein ratio, as evidenced by SDS-PAGE analysis, confirming effective AAV8 capture and elution. Furthermore, the resin demonstrated robust performance across repeated cycles, retaining 71.9 % of its initial binding capacity after 20 uses and maintaining stability with only a 6 % reduction after 7 days at 37 °C. These findings highlight LQ01's potential for scalable and cost-effective AAV8 purification, while demonstrating the broader applicability of Nbs in affinity chromatography and biotechnological processes.

## 1. Introduction

The swift progress in biomedical technologies has led to the emergence of new and potent treatments for human diseases. Specifically, breakthroughs in genetic engineering have facilitated the creation of effective gene therapies utilizing Adeno-associated viruses (AAVs) for a range of diseases [1]. AAVs are efficiently employed in treating both genetic and acquired diseases, particularly monogenic hereditary disorders, which are caused by single gene mutations due to their ability to transduce a variety of cell types with high efficiency and safety. To date, eight AAV vector biologics have received approval [2–4], while numerous other AAV-based gene therapies are currently under investigation in both preclinical and clinical trials.

AAVs are categorized into new serotypes or variants according to serological reactions and amino acid homology [5]. Isolated from rhesus monkey tissue in 2002, AAV8 exhibits high homology with other AAVs. AAV8 demonstrates strong tropism and superior transduction efficiency in liver, as well as muscle and central nervous system, surpassing other serotypes in strength and speed [6]. Its high transduction efficiency and relatively low immunogenicity contribute to its favorability in therapeutic applications [7,8]. Consequently, AAV8 has been extensively utilized in treating metabolic liver diseases, muscle-related disorders, and cardiovascular conditions [9]. However, the development of efficient purification methods for AAV8 remains a critical challenge due to the virus's low natural abundance and the stringent requirements for producing high-purity viral preparations [10].

The promising applications have markedly elevated the demand for AAV8 production and purification. Diverse adaptable methods, including cesium chloride (CsCl) [11] and iodixanol gradient centrifugation (IOD) [12], have been devised for the swift and scalable purification of AAV8. Nonetheless, traditional techniques are laborious, challenging to scale, and necessitate meticulous handling [13].

* Corresponding author. Shanghai Novamab Biopharmaceuticals Co., Ltd. Building No. 10, Lane 500, Furonghua Road, Pudong New District, Shanghai, China.
*E-mail address:* ykwan@novamab.com (Y. Wan).
[1] Guanghui Li and Xiaofei Li contributed equally to the study.

https://doi.org/10.1016/j.pep.2024.106638
Received 30 September 2024; Received in revised form 25 November 2024; Accepted 1 December 2024
Available online 3 December 2024

Recently, single-step affinity column protocols, leveraging antibody specificity, have gained prominence as essential tools for accelerating AAV purification while ensuring compliance with GMP standards [14].

Affinity chromatography is widely acknowledged as an effective technique, but its implementation has been hindered by the unavailability of resins or methods that can purify efficiently without tailored optimization [13,15,16]. The principal advantages of chromatographic purification are its scalability to handle larger volumes and the decreased necessity for manual labor, which significantly cuts costs and streamlines AAV production. Chromatographic resins can be scaled to process substantial volumes, facilitating the input of large, unconcentrated lysate quantities. This process can be automated and meticulously regulated, monitored, and quantified, thereby simplifying troubleshooting and delivering detailed data on the run's quality. As a result, chromatography-based techniques have become fundamental in the industrial production of biologics and small molecules [17].

Due to their remarkable specificity, antibodies are the preferred choice for affinity ligands [18,19]. However, the large size, tetrameric structure, inadequate specificity, reduced stability and high production costs restrict the application as chromatography ligands for targeting of AAVs [20]. Nanobody (Nb)-derived from camelid heavy-chain antibodies-provide high specificity, exceptional stability and are distinguished by their smaller size, thermal stability, refoldability, and pH tolerance [21]. Furthermore, Nbs can be stably expressed with high yields in yeast at relatively low costs [22]. Nb-based immunosorbents have been designed for the purification of various antigens, such as blood endotoxins [23], hormones [24], enzymes [25] and antibodies [26,27]. Nbs, due to their robustness and versatility, offer a viable alternative that can potentially overcome existing limitations and enhance the performance of affinity chromatography [28–30]. Commercially available Nb-based immunoaffinity ligands, such as POROS™ CaptureSelect™ AAVX, AAV8 (CSAL8) and AAV9 (CSAL9), AVB Sepharose HP, Capto™ AVB, and AVIPure™ AAV2, AAV8, AAV9 resins are widely used for AAV purification. Among these, only CaptureSelect™ AAVX, CaptureSelect™ AAV8 and AVIPure™ AAV8 are suitable for AAV8 purification. While CaptureSelect™ AAVX is a broad-spectrum resin that captures various AAV serotypes, its lack of selectively for AAV8 leads to lower purity and necessitates additional purification steps. Furthermore, challenges such as nonspecific binding, cross-reactivity, scalability limitations, and high costs reduce its suitability for high-purity applications. In contrast, CaptureSelect™ AAV8 and AVIPure™ AAV8, being AAV8-specific, offer superior serotype specificity, enhanced purity, higher yields, fewer purification steps, reduced processing costs, and improved scalability. However, as gene therapy progresses, there is a growing need for optimized AAV8-specific nanobody resins that can further improve purity, cost-effectiveness, and scalability for large-scale AAV8 vector production. The development of such resins represents a significant advancement beyond the current state of the art, addressing the existing limitations in specificity, scalability, and cost efficiency.

This study aimed to develop a specialized affinity resin targeting AAV8 by leveraging the advantages of Nbs, offering higher stability and lower cost, and presents an efficient process for developing affinity chromatography resins. Initially, Nbs specific to AAV8 were developed to identify suitable molecules for large-scale capture of AAV8. AAV8-specific Nbs were selected based on their good binding activity in and stability under various pH conditions. These Nbs were conjugated to agarose resins via cysteine at the C-terminal to create affinity chromatography resins. The ligand density of the Nbs conjugated to agarose was assessed. Additionally, the purification efficacy of the resin was evaluated. It was anticipated that the Nb resin would serve as a valuable tool for one-step AAV8 purification and provide a foundation for developing immunoaffinity chromatography for commercial applications.

## 2. Materials and methods

### 2.1. Camel immunization and VHH library construction

AAV8 was sourced from WZ Biosciences (Jinan, China). For each immunization, purified AAV8 at a titer of 7E13 was mixed with Freund's adjuvant and then injected into a healthy, two-year-old Bactrian camel. Following seven weekly immunizations, 100 mL of blood was collected for library construction. All procedures complied with the ethical guidelines of the Shanghai Science and Technology Committee (STCSM).

Peripheral blood lymphocytes (PBLs) were isolated, and total RNA was extracted and reverse-transcribed to cDNA. VHHs were generated using a two-step nested PCR. Purified VHH fragments were subcloned into the phagemid pMECS vector and used to construct phage-display libraries. Library quality was assessed by size and VHH fragment insertion rate.

### 2.2. Biopanning of AAV8-specific Nbs

The AAV8-specific VHHs were selected using phage display. Following three consecutive rounds of bio-panning, 300 individual colonies were randomly chosen to identify specific Nbs through periplasmic extract enzyme linked immunosorbent assay (PE-ELISA). The sequences of these Nbs were analyzed using software MEGA.

### 2.3. Expression and purification of Nbs

After sequencing the selected clones, AAV8-specific clones were amplified, and their plasmids were isolated and introduced into *Escherichia coli* (*E. coli*) strain WK6. Immobilized metal ion affinity chromatography (IMAC) was utilized for the purification of Nbs. Sodium dodecyl sulfate-polyacrylamide gel electrophoresis (SDS-PAGE) was employed to confirm the purity of the Nbs.

### 2.4. Binding activity detection

The ELISA was used to assess AAV8 binding. Microplates were coated with AAV8 overnight at 4 °C, then washed five times with PBST and blocked with 1 % BSA at 37 °C for 2 h. Nbs (2 μg/mL in 1 × PBS) were added and incubated at 37 °C for 1 h. After five additional PBST washes, mouse anti-His-HRP antibody was added and incubated at 37 °C for 1 h. The reaction was developed with TMB buffer and stopped with 2M $H_2SO_4$. Absorbance at 450 nm was measured. To identify suitable candidates, the binding capacity of Nbs to AAV8 can be assessed under different reaction buffer conditions.

### 2.5. Expression of Nbs by Pichia pastoris

The VHH gene vector was linearized and introduced into *Pichia pastoris* to develop a high-efficiency expression system. Dozens of clones were screened in shake flasks. After identifying the high expression clone, large-scale expression was carried out in 7-L bioreactor using our standard fermentation method. During the fermentation process, broth samples were collected at various times, centrifuged at 12,000 rpm for 5 min, and analyzed by SDS-PAGE. The supernatants of different fermentation time were tested by SDS-PAGE. The titer of supernatants was tested using Fortebio's Octet RED96 instrument (ForteBio, Menlo Park, CA, USA).

### 2.6. Purification and specificity confirmation of Nb9

#### 2.6.1. IMAC

IMAC was conducted using Ni Sepharose Excel resin (Cytiva, Sweden) within a 25 × 60 mm column. The culture supernatant containing the target protein Nb9 was applied at a maximum loading capacity of 20

mg/mL. The column was equilibrated with a buffer solution consisting of 20 mmol/L phosphate buffer (PB) and 0.5 mol/L NaCl at pH 7.4. Elution was performed using the same buffer supplemented with 0.5 mol/L imidazole.

#### 2.6.2. Size-Exclusion Chromatography (SEC)

Subsequent purification of the Ni-affinity captured Nb9 was achieved through size-exclusion chromatography using SRT-C SEC-300 resin (Sepax, China) in a 21.2 × 300 mm column. The column was equilibrated with a buffer of 0.1 mol/L $NaHCO_3$ and 0.5 mol/L NaCl at pH 7.4. The column was equilibrated with a buffer containing 0.1 mol/L $NaHCO_3$ and 0.5 mol/L NaCl at pH 7.4, after which Nb9 was loaded at a maximum concentration of 42 mg. Elution was performed using the same buffer used for equilibration.

### 2.7. Conjugation of Nb9 with different resin

To determine the optimal resin for conjugating with Nb9, two primary types of resin were evaluated: Epoxy activated Bestarose 6B (Bestchrom, China) and PabPur SulfoLink Beads 4FF (Smart-Lifesciences, China). Prior to conjugation, Nb9 was treated with 10 mM tris (2-carboxyethyl) phosphine (TCEP) at room temperature for 2 h. The mixture was then exchanged into the conjugation buffer separately and concentrated to a final concentration exceeding 10 mg/mL.

#### 2.7.1. Epoxy activated Bestarose 6B

The resin was rinsed with purified water and subsequently washed with conjugation buffer (0.1 M $NaHCO_3$ and 0.5 M NaCl, pH 9.5) at a volume five times that of the resin, then drained. After exchanging the buffer, Nb9 was added, mixed thoroughly, and allowed to incubate overnight at room temperature. Following incubation, the protein solution was removed, and the resin was rinsed three times with conjugation buffer. Subsequently, 1 M ethanolamine was added, and the reaction was allowed to shake overnight at room temperature. The resin was then rinsed with purified water and preserved.

#### 2.7.2. PabPur SulfoLink Beads 4FF

The resin was similarly washed with purified water and equilibrated with conjugation buffer (50 mM Tris, 5 mM EDTA-Na, pH 8.5) at a volume five times that of the resin, then drained. The Nb9 solution was added to the conjugation resin, thoroughly mixed, and incubated at room temperature for 30 min. After incubation, the protein solution was removed, and the resin was washed three times with conjugation buffer, then drained. A termination solution (50 mM Tris, 5 mM EDTA-Na, 50 mM L-cysteine, pH 8.5) was added to quench the reaction before the resin was preserved.

### 2.8. Buffer optimization for static binding capacity of LQ01 resin

The effects of equilibration buffer on the static binding capacity of LQ01 resin were evaluated under a pH range from 3.0 to 8.0 and NaCl concentrations ranging from 0 to 2.0 M. The impact of pH on the binding capacity was assessed by preparing 20 mM phosphate buffers adjusted to pH values of 2.0, 3.0, 4.0, 5.0, 6.0, 7.0, and 8.0. For ionic strength evaluation, NaCl was added to the 20 mM phosphate buffer (pH 7.0) to achieve final concentrations of 0, 0.15, 0.5, 0.75, 1.25, 1.50, 1.75 and 2.0 M.

The static binding capacity was determined through batch experiments. Empty 5 mL tubes were loaded with 0.4 mL of a 50 % slurry of LQ01 resin and centrifuged for 30 s at 5,000×*g* to remove the supernatant. The resins were washed with 4 mL of equilibration buffer at the designated pH or NaCl concentration. Pre-purified AAV8 in the same buffer was added to each tube and incubated on a shaker at 25 °C for 30 min. The tubes were then centrifuged for 30 s at 5,000×*g*. The concentration of AAV8 in the supernatant was determined using an AAV8-specific ELISA kit.

The static binding capacity (SC, vp/mL) was calculated using the following equation:

$$SC = \frac{(C0 - C1) \times V}{0.2}$$

where C0 and C1 represent the concentrations of AAV8 before and after incubation, respectively, and V is the volume (mL) of pre-purified AAV8 added.

This methodology enabled a comprehensive analysis of the impact of pH and ionic strength on the binding efficiency of LQ01 resin, providing critical insights for optimizing buffer conditions during AAV8 purification.

### 2.9. Capsid quantification via AAV8 titration ELISA kit

The AAV8 concentration in feed, flow-through, and elution fractions was quantified utilizing the AAV8 titration ELISA kit (PROGEN, Wayne, PA) in accordance with the manufacturer's guidelines.

### 2.10. Evaluation of the purification effect of LQ1 resin

The purification of the AA8 sample by LQ01 resin was evaluated using an AKTA Explorer (Cytiva, Sweden) chromatography system equipped with a 1 mL pre-packed column. Column volume (CV) for the purification was set as 1 mL regardless of the actual volume of the LQ01 resin used. Equilibration, washes, elute and regeneration of the column were performed at a rate of 2 mL/min. The retention time was 5 min. The column was equilibrated with 5 CV of Buffer A (20 mmol/L PB and 150 mmol/L NaCl, pH 7.0). The fermentation supernatant of AAV8 was loaded onto the column by a volume of 10 mL. Next, the first wash was performed using 5 CV of Buffer A, followed by a second wash with 5 CV of Buffer B (20 mmol/L PB and 1 mol/L NaCl, pH 7.0), and finally a third wash was conducted with 5 CV of Buffer C (20 mmol/L PB, pH 7.0). Afterward, elution was carried out by 5 CV of Buffer D (50 mmol/L Gly-HCl and 20 % propylene glycol, pH 3.0). Resin was then regenerated with 5 CV of Buffer E (1 M acetic acid) and washed again with 5 CV Buffer A. The fractions of flow-through, wash (Buffer B), elution (Buffer D) and regeneration (Buffer E) were collected separately for SDS-PAGE detection.

## 3. Results

### 3.1. Construction of immunized phage display Nb library

To generate Nbs with high affinity and specificity for AAV8, a 2-year-old healthy Bactrian camel was immunized with AAV8 over 7 weeks After the final immunization, antigen-specific total IgG titers in the camel's serum were evaluated, revealing a strong signal at a 1:10000 dilution. This indicated a successful immunization and robust immune response to AAV8. Subsequently, an AAV8-specific VHH library was constructed using a two-round PCR to amplify the heavy chain antibody variable region. As shown in Fig. 1A, the first PCR produced fragments around 700 bp, while the VHH-only region products were approximately 400 bp. Verified VHH fragments were then ligated into the pMECS vector and transformed into TG1 *E. coli* cells, which were plated to generate the VHH library. Library size and insertion rate reflect its quality. The VHH library against AAV8 was estimated to contain approximately 5E9 colony-forming units (CFU), suggesting sufficient specificity and sequence diversity (Fig. 1B). The insertion rate was evaluated by PCR analysis of 24 randomly selected clones (Fig. 1C). The 100 % insertion rate confirmed the successful construction of a high-quality, diverse VHH library against AAV8, providing a solid foundation for screening high-quality Nbs.

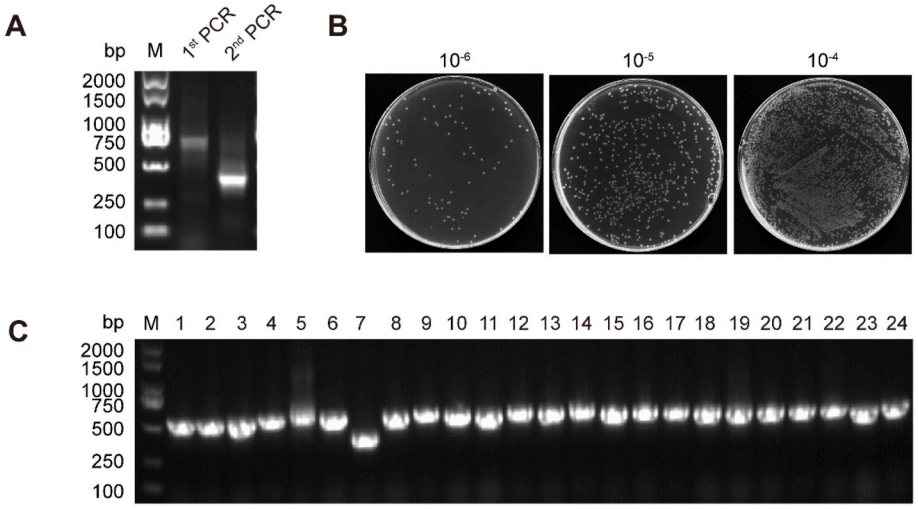


**Fig. 1.** Construction of anti-AAV8 phage displayed library. (A) Segments containing VHH gene fragments were amplified through a two-round PCR process. (B) The library capacity was determined by counting colonies on plates after gradient dilution. (C) The correct insertion rate was estimated by performing PCR on 24 randomly selected colonies.

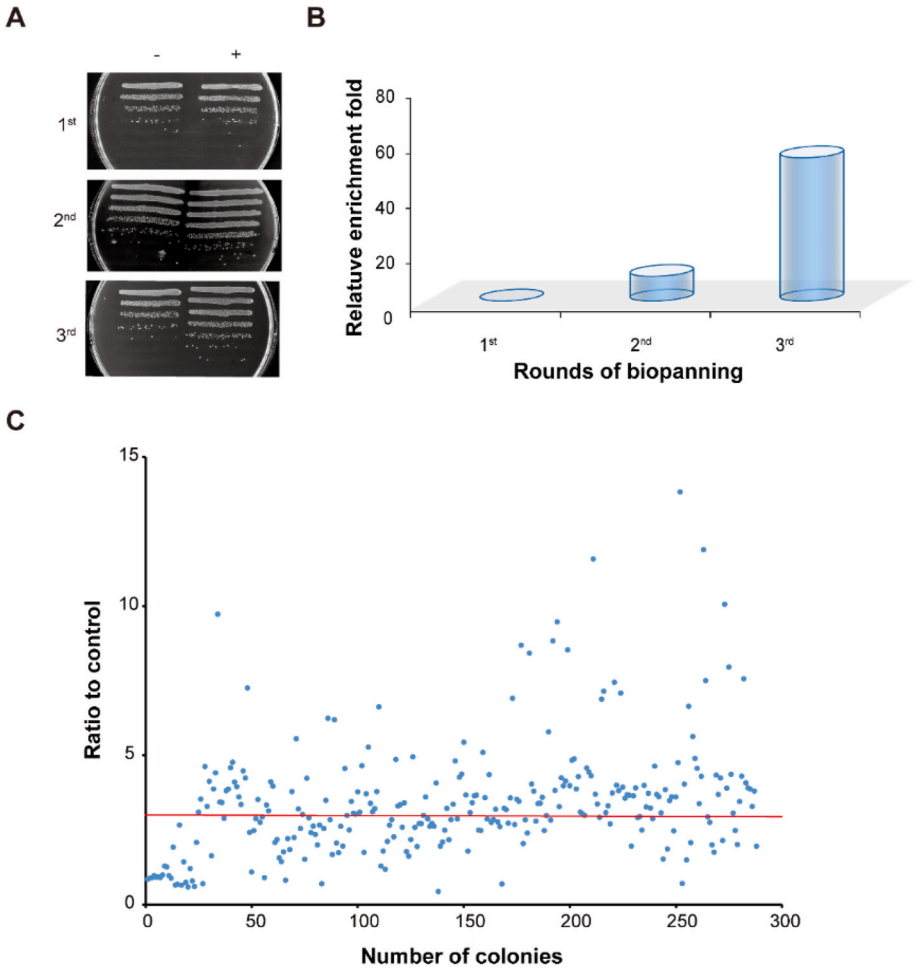


**Fig. 2. AAV8-specific VHH genes were derived from the phage display library**. (A) The phage particles' enrichment in antigen-coated wells was measured against uncoated wells after each panning cycle. (B) Following three panning cycles, AAV8-specific VHHs demonstrated a 58-fold increase in enrichment compared to the control wells (±). (C) Periplasmic extract ELISA was performed on 300 colonies. Colonies with absorbance signals more than three times higher than the negative control were marked as positive.

### 3.2. Selection of AAV8-specific Nbs via phage display bio-panning

Phage display technology was utilized to identify AAV8-specific Nbs through bio-panning. As indicated in Fig. 2A and B, a three-round screening resulted in a 58-fold increase in the enrichment of targeted phages. Following this, approximately 300 colonies were selected at random from the bio-panning rounds and subjected to periplasmic extraction enzyme-linked immunosorbent assay (PE-ELISA). Out of these, 177 colonies demonstrated a binding ratio exceeding 3 in comparison to the blank control (Fig. 2C). Sequence analysis and alignment revealed nine distinct sequences, which were categorized into separate groups based on the variation in their complementarity determining region (CDR)3 amino acid sequences, designated as Nb1 to Nb9. These nine candidate Nbs will subsequently undergo expression and purification for further investigation.

### 3.3. Expression of the Nbs and binding activity to AAV8 in different conditions

The plasmids encoding the identified nine Nbs were introduced into the WK *E. coli* strain, enabling the expression of soluble Nbs via the amber stop codon. The purified Nbs, isolated via Ni−NTA chromatography, were characterized by SDS−PAGE, revealing a molecular mass of approximately 15 kDa and a purity of exceeding 95 % (Fig. 3). The observed molecule weight aligned with the theoretical prediction and the high level of purity permitted subsequent affinity assays.

### 3.4. Screening of Nb candidates under simulated affinity resin development conditions

The selection of nine candidates for affinity chromatography development was achieved through a detailed evaluation of their binding activities under simulated real-world conditions. To enhance the selection process, a range of critical conditions was employed. Binding assessments were performed at pH 7 to reflect physiological conditions. For elution studies, pH values of 3.0, 3.5, and 4.0 were used, which are commonly employed to disrupt antibody interactions. Additionally, the Nbs' durability in alkaline environments was examined using clean-in-place (CIP) with 0.1M NaOH, a standard practice to ensure contaminant removal and maintain resin integrity. Furthermore, antibody stability was evaluated through storage in 20 % ethanol.

By examining the variations in binding activity across these conditions, Nbs exhibiting superior and consistent performance were identified. Fig. 4 illustrates that Nb4, Nb5, and Nb9 demonstrated strong binding affinity at pH 7 and in 20 % ethanol. However, these candidates showed markedly reduced or negligible binding at pH 3.0, 3.5, 4.0, and 0.1M NaOH. This thorough screening approach was instrumental in selecting Nbs that not only exhibit efficacy under optimal conditions but also display resilience across a spectrum of conditions encountered in downstream bioprocessing. The optimized screening process provides a solid research foundation for developing AAV8-specific affinity media, ensuring that future efforts in creating effective affinity chromatography materials will be based on well-characterized Nbs with proven performance.

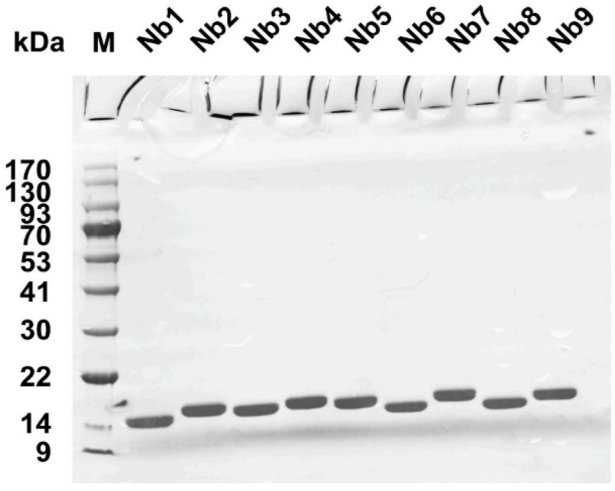


**Fig. 3. The reduced SDS-PAGE gel analysis of AAV8-specific Nbs**. M: Marker; Lanes 2–10: Purified nine anti-AAV8 Nbs, respectively. All proteins were separated on a 15 % SDS-PAGE gel and stained with Coomassie Brilliant Blue.

### 3.5. Optimized expression for Nbs in P. pastoris

*P. pastoris* provides high expression efficiency and effective post-translational modifications for Nbs. Its scalability, cost-effectiveness, and optimized conditions ensure high yields and consistent quality, making it ideal for both research and industrial use.

Nbs targeting AAV8 were developed by cloning genes encoding Nb4, Nb5, and Nb9 into expression vectors and electrotransforming them into *P. pastoris* with a C-terminal cysteine tag. High-yield clones were selected via antibiotic resistance screening and expression assays in 24-well plates. Following fermentation, clarification, and purification, the Nbs were obtained, as shown in Fig. 5A.

The three candidate Nbs expressed in 24-well plates by *P. pastoris* were analyzed by SDS-PAGE, as shown in Fig. 5B. Non-reducing SDS-PAGE revealed two bands for Nb4, Nb5, and Nb9: a monomer and a dimer (Fig. 5B, lanes 1, 3, and 5). Reducing SDS-PAGE displayed bands around 15 kDa, consistent with the theoretical molecular weights of Nb4, Nb5, and Nb9 (Fig. 5B, lanes 2, 4, and 6). Meanwhile, we determined that Nb9 has the highest expression titer compared to Nb4 and Nb5.

Large-scale, cost-effective Nb production is essential for future commercial applications. High expression yields are crucial for selecting Nbs or affinity ligands, affecting production efficiency and cost. Additionally, robust expression indicates favorable protein characteristics, including proper folding and stability, which are vital for downstream applications. Therefore, Nb9, the highest-yielding candidate, was expressed in a 7 L fermenter using *P. pastoris*. During fermentation in the 7 L fermenter, the yield of Nb9 protein improved. As depicted in Fig. 5C, the SDS-PAGE analysis of supernatant samples from the 7 L fermenter indicated a progressive increase in Nb9 concentration over time. Additionally, Fig. 5D illustrates that the wet cell weight reached 456 g/L, and the yield of the target protein in the fermentation supernatant achieved 7 g/L following 161 h of induction in the 7 L bioreactor, consistent with the results obtained from the SDS-PAGE analysis (Fig. 5C).

### 3.6. Purification and binding activity confirmation of Nb9

To acquire purified protein for AAV8 affinity chromatography resin preparation, the supernatant containing Nb9 (tagged with an N-terminal His6) from a 7L fermenter was sequentially processed through IMAC resin followed by size-exclusion chromatography (SEC). The purification chromatograms for the two steps were presented in Fig. 6A and B. The yield from the IMAC and SEC processes were 60.1 % and 60.7 %, respectively (Table 1). The fractions from IMAC and SEC were analyzed by SDS-PAGE, as depicted in Fig. 6C. Since Nb9 molecules contain free sulfhydryl groups, disulfide bonds can form automatically between some Nb9 molecules, resulting in dimer. Consequently, the Nb9 solution contains both monomers and dimer in the absence of any special treatment. The non-reduced SDS-PAGE revealed two bands in the fractions, indicative of the monomer and dimer forms (Fig. 6C, lanes 1 and 3). Under reducing conditions, a protein band of approximately 15 kDa was observed on the SDS-PAGE gel, aligning with the theoretical molecular weight of Nb9 (Fig. 6C, lanes 2 and 4). Compared to the IMAC

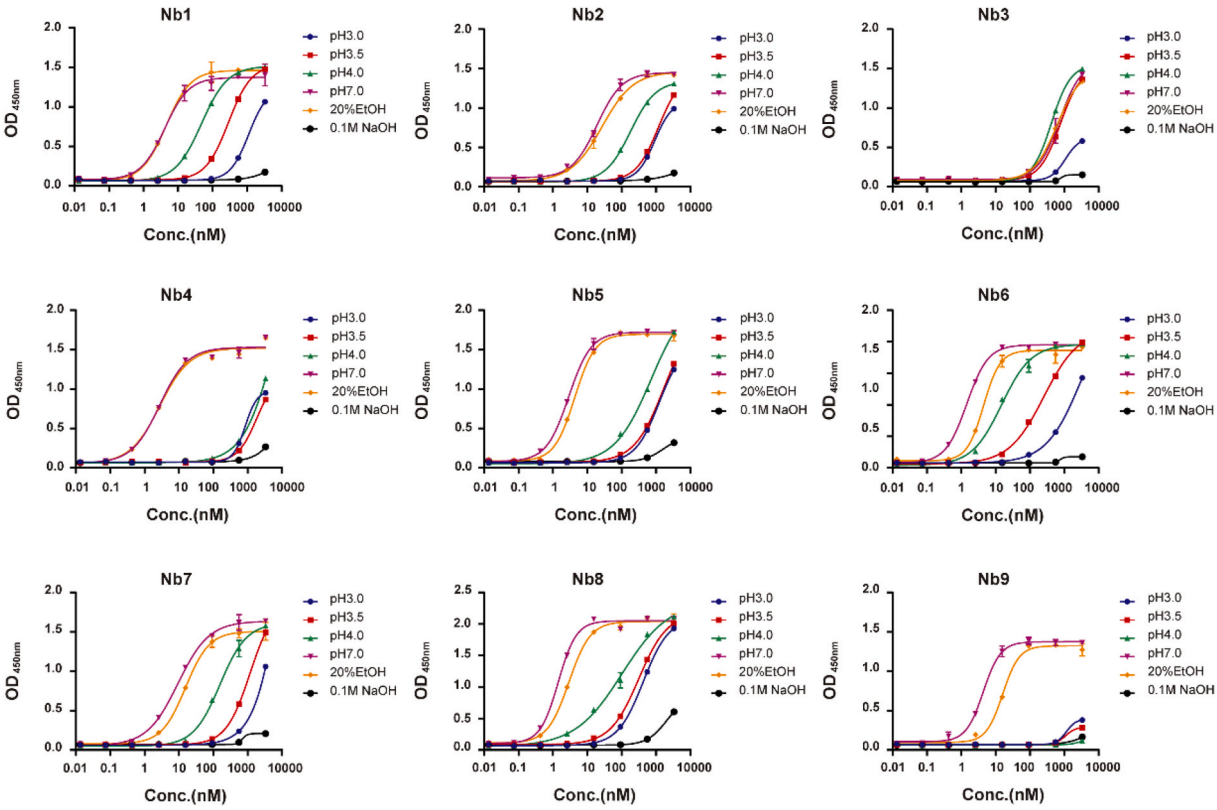


**Fig. 4.** The binding capacity of Nbs to AAV8 under simulated affinity resin development conditions.

product, the purity of the SEC collection was significantly improved. The SEC-purified Nb9 was utilized in subsequent assays. The binding affinity of Nb9, produced in *P. pastoris* and reduced by ECTP, assessed across various pH levels, as demonstrated in Fig. 6D. The ELISA binding assay confirmed that Nb9 effectively binds to AAV8 at pH 7.0, with an EC50 value of 2.292 nM. Additionally, Nb9 dissociates from AAV8 effectively at pH 3.0.

### 3.7. Conjugation of Nb9 with different resin

Two types of agarose microspheres were selected for Nb9 conjugation: Epoxy activated Bestarose 6B and PabPur SulfoLink Beads 4FF, each utilizing distinct coupling principles. Epoxy activated Bestarose 6B is a pre-activated filler that anchors ligands by facilitating the coupling of hydroxyl, amino, or sulfhydryl groups to the agarose gel. In contrast, PabPur SulfoLink Beads 4FF are also pre-activated microspheres but are specifically designed to immobilize antigens through reactions with sulfhydryl groups alone, enabling antibody purification.

Nb9 was immobilized onto Epoxy activated Bestarose 6B resin through an epoxy-based covalent coupling reaction (Fig. 7A), as previously described. Additionally, Nb9 was conjugated to PabPur SulfoLink Beads 4FF resin via a cysteine residue at the C-terminal, forming affinity chromatography resins (Fig. 7B). The ligand densities were determined to be 9.12 mg/mL for the Epoxy activated Bestarose 6B resin and 0.35 mg/mL for the PabPur SulfoLink Beads 4FF resin, respectively. This substantial difference in ligand density is pivotal in the development of affinity chromatography resins, with the higher density in the Epoxy activated Bestarose 6B resin, selected for further development into LQ01 (Nb9 as affinity ligand coupled with Epoxy activated Bestarose 6B resin), indicating a potential for superior binding capacity and purification efficiency. These findings have direct implications for the resin's performance, influencing factors such as binding efficiency, specificity, and overall yield, which are critical for evaluating its suitability for large-scale and commercial applications. The LQ01 resin was subsequently packed into a 1 mL column for use in the following purification steps.

### 3.8. Effects of buffer on the binding of AAV8 to LQ01 resin

Assessing buffer pH and ionic strength is crucial for elucidating their impact on the binding and elution characteristics of affinity resins, enabling precise process optimization and ensuring consistent resin performance. The buffer's pH and ionic strength were evaluated to determine their effects on LQ01 resin binding capacity. LQ01 demonstrated maximum static binding capacity at pH 7.0, which progressively diminished at both lower and higher pH levels, reaching its lowest point around pH 3.0 (Fig. 8A). This trend corresponded with the Nb9 screening data, confirming the pH sensitivity of the interaction between Nb9 and AAV8. The influence of ionic strength on LQ01 resin binding capacity was assessed by introducing NaCl into a 20 mM phosphate buffer (pH 7.0) at concentrations ranging from 0 to 2.0 M. As shown in Fig. 8B, the binding capacity remained relatively stable between 0 and 1.0 M NaCl, with an optimal value observed at 0.15 M. Therefore, 0.15 M NaCl was selected as the equilibration buffer for initial balancing and preliminary washing steps. However, a significant decrease in binding capacity was noted at NaCl concentrations exceeding 1.25 M, indicating that higher ionic strength may disrupts the interaction between the Nb9 ligand and AAV8, possibly affecting both the ligand-virus and ligand-resin interactions. These findings highlight the critical role of pH and buffer ionic strength in optimizing binding and elution conditions for LQ01 resin, ensuring robust performance during AAV8 purification, ultimately improving process efficiency and product purity.

### 3.9. Evaluation of purification performance of LQ01 resin from crude lysates

To determine the effectiveness of the LQ01 resin for AAV8 purification, a comprehensive purification process was carried out using the supernatant. The chromatogram of the purification process with LQ01

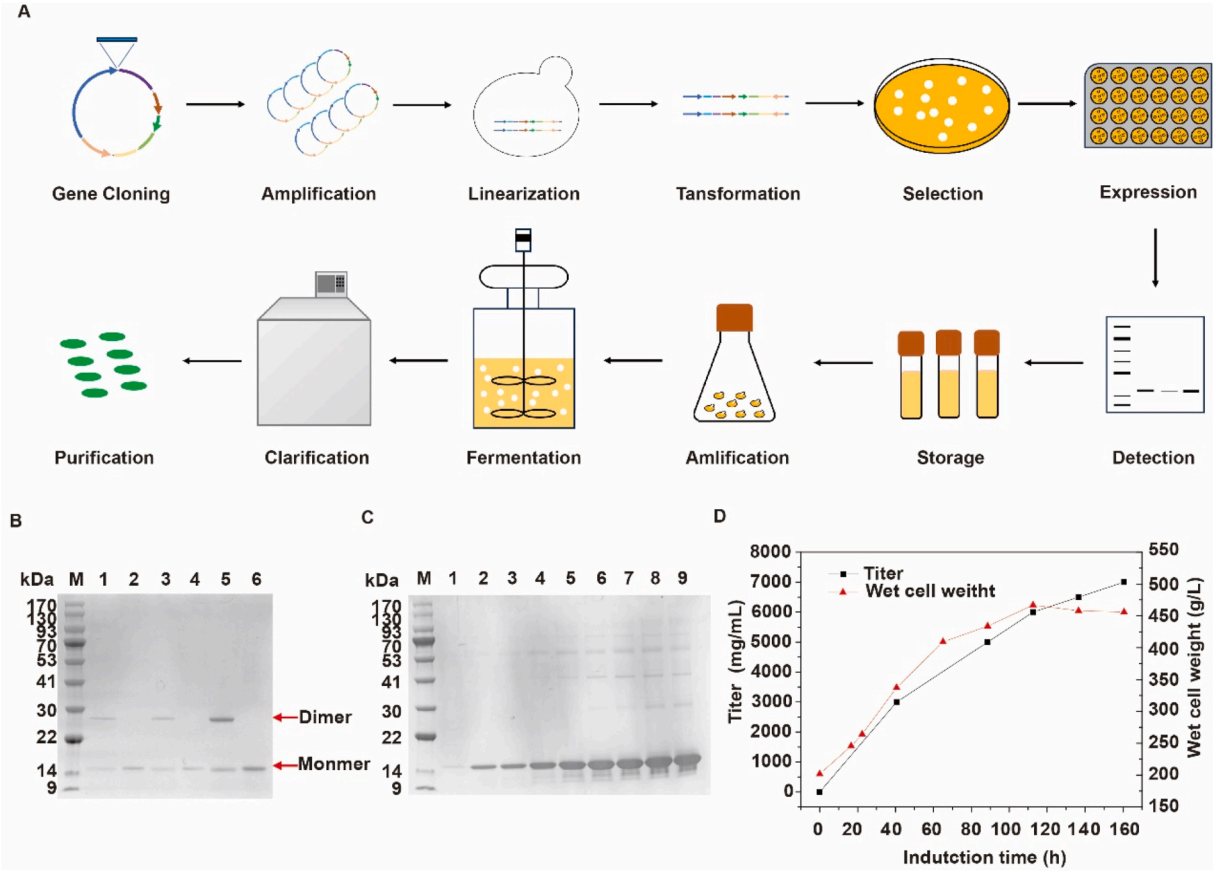


**Fig. 5. Expression of Nbs by *P. pastoris*.** (A) Flow chart of Nb preparation. (B) Reducing and non-reducing SDS-PAGE analysis. M, prestained molecular weight markers; lanes 1, 3, 5: 10 μL non-reducing culture supernatants of Nb4, Nb5 and Nb9 after 48 h induction. lanes 2, 4, 6: 10 μL reducing supernatants of Nb4, Nb5 and Nb9 after 48 h induction. (C) Reducing SDS-PAGE analysis of Nb9 produced in a 7L bioreactor; lanes 1–9, 1.6 μL culture supernatants after 0, 17, 22, 41, 65, 89, 113, 137 and 161 h of induction. (D) Wet cell weight and titer during Nb9 fermentation in a 7L bioreactor.

resin is shown in Fig. 9A. Various samples collected during the purification process, including Load, Flow-through 1, Flow-through 2, Wash, Elution 1, Elution 2, and Regeneration 1, were analyzed using SDS-PAGE to assess the relative purity (Fig. 9B).

Compared to lane 1 in Fig. 9B, which represents the initial supernatant, lane 2 demonstrates a significant reduction in AAV8 content, indicating successful binding of AAV8 to the LQ01 resin. This suggests that the resin effectively captures AAV8 from the supernatant. Analysis of Elution 2 (Fig. 9B, lane 6) displayed distinct VP1, VP2, VP3 bands with minimal non-specific bands, closely aligned with the theoretical ratio of 1:1:10. This indicates that the LQ01 resin achieves high purity, effectively removing impurities while maintaining the structural integrity of the AAV8 capsid. The high purity of the eluted AAV8 particles highlight the resin's robustness and reliability, making it suitable for large-scale biopharmaceutical applications such as gene therapy and vaccine production.

### *3.10. Reusable and stability of LQ01 resin*

Reusability and stability are critical characteristics of affinity resins, particularly in downstream processing within the biopharmaceutical industry. The stability of LQ01 upon repeated use was evaluated. As shown in Fig. 10A, a steady decline in binding capacity was observed over multiple cycles of use, with the static binding capacity of LQ01 remaining approximately 71.9 % of the original after 20 cycles. The loss of binding capacity with use is attributed to several factors, including chemical degradation due to harsh acidic conditions, physical damage, and fouling. Additionally, a 7-day storage test at 37 °C was conducted on LQ01, demonstrating its good stability (Fig. 10B), with a 6 % decrease in binding capacity.

## 4. Discussion

This study successfully established phage display Nb library specifically targeting AAV8, identifying nine candidates with high specificity and affinity through simulated screening. The generation of a high-quality Nb library, utilizing a two-round PCR approach, yielded approximately 5E9 CFU, ensuring both specificity and diversity. This robust library lays a solid foundation for the development of highly specific single-domain antibodies.

During the selection process, phage display technology enabled a substantial enrichment of target phages, while ELISA validation revealed a high binding activity among 177 selected clones. Notably, Nb4, Nb5, and Nb9 demonstrated excellent binding characteristics under physiological conditions, alongside good resilience in simulated cleaning scenarios. These findings underscore the practical applicability of these Nbs in bioprocessing, enhancing our ability to select nanobodies that perform well across diverse conditions, thereby facilitating the future development of affinity chromatography resin.

Further, we optimized the expression for Nbs in *P. pastoris*, achieving high expression yields and effective purification. Among the candidates, Nb9 exhibited the highest expression levels, which were notably superior to those of other candidates. The binding affinity of Nb9 across various pH conditions, further supports its potential for downstream applications.

In the context of immobilization, we compared two types of agarose microspheres, revealing that Epoxy-activated Bestarose 6B had a significantly higher ligand density of 9.12 mg/mL than PabPur SulfoLink

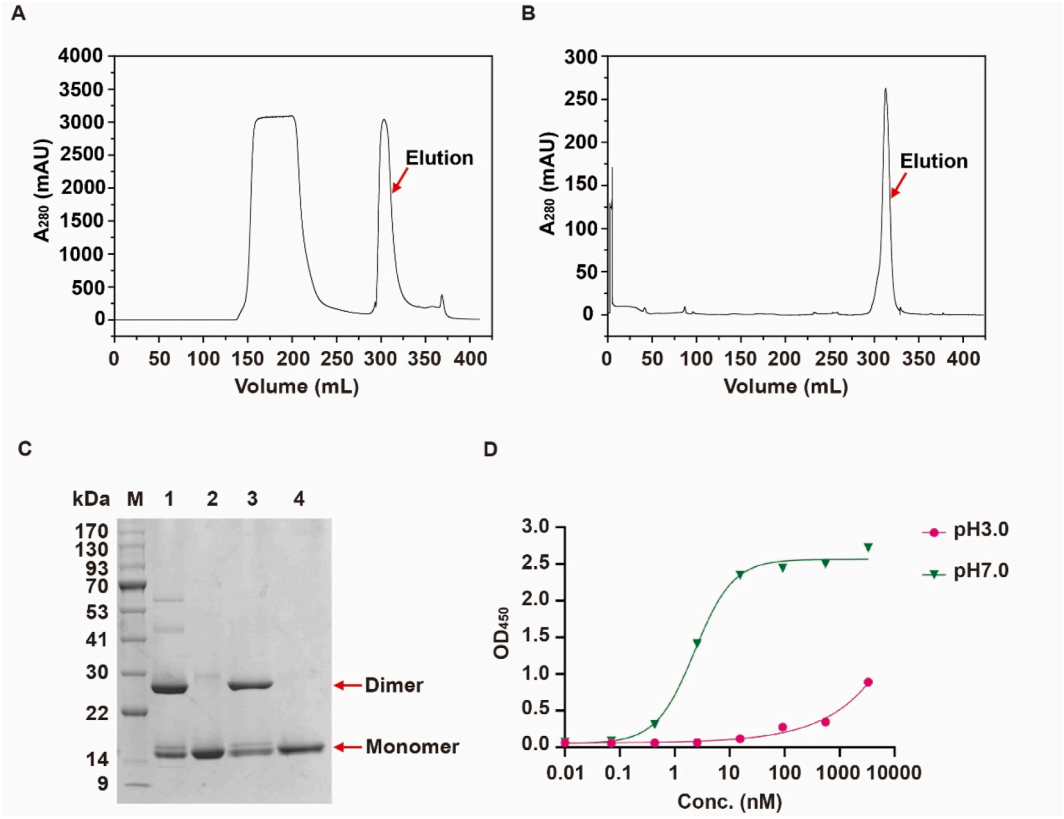


**Fig. 6. Purification and binding activity confirmation of Nb9.** (A) IMAC chromatograms of Nb9. (B) SEC chromatograms of Nb9. (C) SDS-PAGE analysis of Nb9. M, pre-stained molecular weight markers. lanes 1, 3: 5 μg non-reducing harvest solution of IMAC and SEC; lanes 2, 4: 5 μg reducing harvest solution of IMAC and SEC. (D) The binding activity of Nb9 assessed by ELISA.

**Table 1**
Yield of the purification process.

| Step | Loading Volume (mL) | Loaded protein (mg) | Elution Volume (mL) | Eluted protein (mg) | Yield (%) |
|---|---|---|---|---|---|
| IMAC | 50 | 350 | 31.27 | 210.34 | 60.1 |
| SEC | 0.78 | 7.52 | 12 | 4.56 | 60.7 |

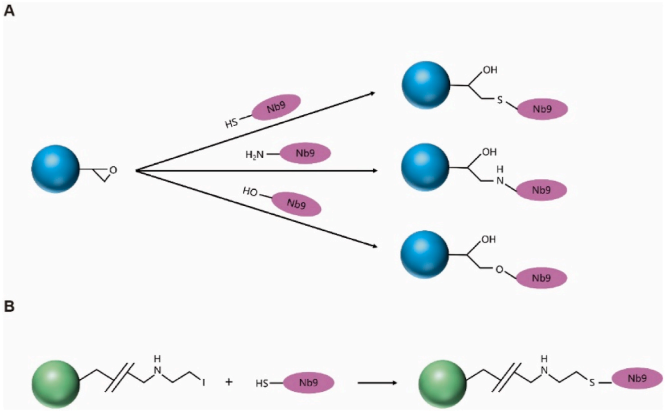


**Fig. 7. General structure and reaction scheme for coupling resin.** (A) Epoxy activated Bestarose 6B. (B) PabPur SulfoLink Beads 4FF.

Beads 4FF of 0.35 mg/mL. The difference in ligand density between Epoxy-activated Bestarose 6B and PabPur SulfoLink Beads 4FF may arises from their distinct coupling mechanisms and resin properties. This discrepancy affects the binding capacity and could have direct implications for purification efficiency. Epoxy-activated Bestarose 6B was a better choice for applications that require enhanced binding capacity and purification efficiency. Future work will focus on optimizing and evaluating the practical applications of LQ01 resin to ensure stability and efficacy in large-scale production.

LQ01 resin, developed from Bestarose 6B, exhibited optimal performance at pH 7.0 and decreased binding at higher ionic strengths, highlighting the need for controlled buffer conditions. Purification trials confirmed LQ01's high specificity and purity in capturing AAV8, crucial for gene therapy applications. Additionally, LQ01 demonstrated good reusability, retaining 71.9 % binding capacity after 20 cycles, and stability, with minimal degradation during storage. These findings affirm LQ01's potential for efficient, scalable AAV8 purification in biopharmaceutical applications.

To evaluate the performance of LQ01 resin in AAV8 purification, we conducted a purification process, analyzing the process samples of different stages. The results indicated a significant reduction in AAV8 content in the supernatant post-binding, confirming the effective capture of AAV8 by the resin. The final elution exhibited clear VP1-VP3 bands with minimal non-specific contamination, demonstrating that LQ01 resin not only binds AAV8 efficiently but also elutes with high specificity and low contaminant levels. These findings highlight the robustness and versatility of the LQ01 resin, capable of selectively isolating and concentrating AAV8, which is crucial for downstream applications in vaccine development and gene therapy. Further research will continue to focus on optimizing its performance to enhance its real-world applicability.

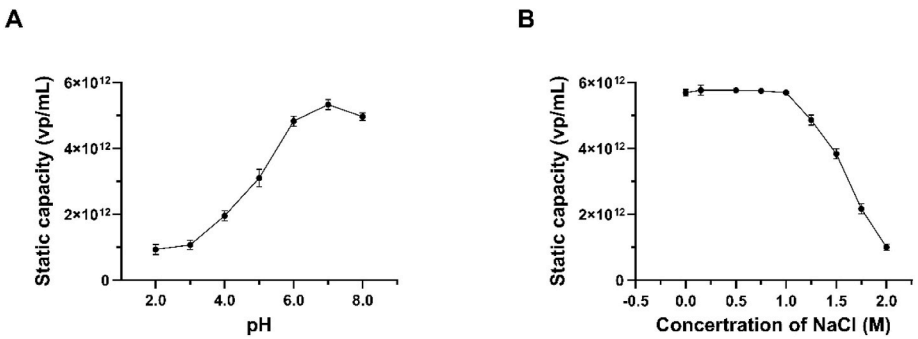


**Fig. 8.** The static binding capacity of LQ01 determined under different pH (A) and NaCl concentration (B). The measurements were performed in triplicates.

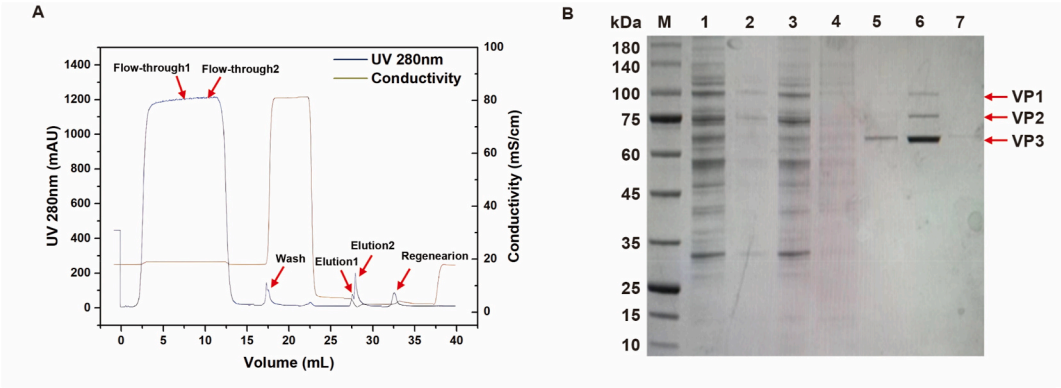


**Fig. 9. Purification process of AAV8 using LQ01 resin**. (A) Chromatogram of the purification process. (B) SDS-PAGE analysis of chromatographic fractions; M, molecular weight markers. lanes 1: Supernatant; lanes 2: Flow-through 1; lanes 3: Flow-through 2; lanes 4: Wash (Buffer B); lanes 5: Elution 1 (Buffer D); lanes 6: Elution 2 (Buffer D); lanes 7: Regeneration (Buffer E).

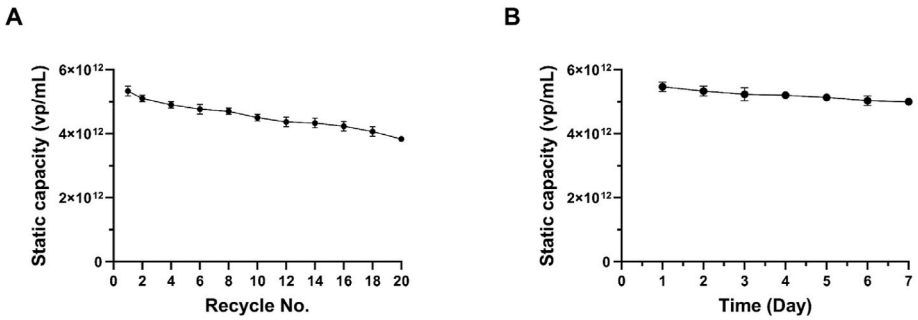


**Fig. 10.** Stability determination of LQ01. (A) Recycling use of LQ01. (B) The static capacity during 7-day storage at 37 °C.

## 5. Conclusions

In conclusion, this study establishes a comprehensive framework for developing specific affinity resin targeting AAV8 while providing valuable insights into the application of Nbs in biotechnology and pharmaceuticals. The LQ01 resin emerges as a promising tool for efficient and cost-effective purification method for AAV8, offering enlightenment and references for affinity chromatography across various products based on Nbs.

## CRediT authorship contribution statement

**Guanghui Li:** Writing – review & editing, Writing – original draft, Visualization, Software, Methodology, Investigation. **Xiaofei Li:** Writing – review & editing, Writing – original draft, Visualization, Software, Methodology. **Min Zhu:** Visualization, Investigation, Formal analysis. **Peng Qiao:** Visualization, Validation, Investigation, Formal analysis. **Weiwei Ji:** Writing – original draft, Visualization, Formal analysis. **Yuping Huang:** Writing – original draft, Visualization, Formal analysis. **Yicai Zhang:** Writing – original draft, Visualization, Formal analysis. **Xuee Li:** Project administration, Formal analysis. **Yakun Wan:** Supervision, Project administration, Methodology, Funding acquisition, Data curation, Conceptualization.

## Declaration of interest

The authors declare that there is no conflict of interests.

## Acknowledgements

This work is financially supported by the Science and Technology Commission of Shanghai Municipality (grant number 23J21901800). The authors sincerely thank Suzhou NanoMicro Technology Co., Ltd. for their essential technological support in Fig. 9 about evaluation the

purification performance of LQ01 resin from crude lysates.

## Data availability

Data will be made available on request.

## References


[1] S.S. Issa, A.A. Shaimardanova, V.V. Solovyeva, A.A. Rizvanov, Various AAV serotypes and their applications in gene therapy: an overview, Cells 12 (5) (2023), https://doi.org/10.3390/cells12050785.

[2] M.C. Ozelo, J. Mahlangu, K.J. Pasi, A. Giermasz, A.D. Leavitt, M. Laffan, E. Symington, D.V. Quon, J.D. Wang, K. Peerlinck, S.W. Pipe, B. Madan, N.S. Key, G.F. Pierce, B. O'Mahony, R. Kaczmarek, J. Henshaw, A. Lawal, K. Jayaram, M. Huang, X. Yang, W.Y. Wong, B. Kim, G.E.-T. Group, Valoctocogene roxaparvovec gene therapy for hemophilia A, N. Engl. J. Med. 386 (11) (2022) 1013–1025, https://doi.org/10.1056/NEJMoa2113708.

[3] Zolgensma - one-time gene therapy for spinal muscular atrophy, Med. Lett. Drugs Ther. 61 (1577) (2019) 113–114.

[4] D.A. Prado, M. Acosta-Acero, R.S. Maldonado, Gene therapy beyond luxturna: a new horizon of the treatment for inherited retinal disease, Curr. Opin. Ophthalmol. 31 (3) (2020) 147–154, https://doi.org/10.1097/ICU.0000000000000660.

[5] Z. Wu, A. Asokan, R.J. Samulski, Adeno-associated virus serotypes: vector toolkit for human gene therapy, Mol. Ther. 14 (3) (2006) 316–327, https://doi.org/10.1016/j.ymthe.2006.05.009.

[6] L. Zhao, Z. Yang, M. Zheng, L. Shi, M. Gu, G. Liu, F. Miao, Y. Chang, F. Huang, N. Tang, Recombinant adeno-associated virus 8 vector in gene therapy: opportunities and challenges, Genes Dis 11 (1) (2024) 283–293, https://doi.org/10.1016/j.gendis.2023.02.010.

[7] A. Kruzik, D. Fetahagic, B. Hartlieb, S. Dorn, H. Koppensteiner, F.M. Horling, F. Scheiflinger, B.M. Reipert, M. de la Rosa, Prevalence of anti-adeno-associated virus immune responses in international cohorts of healthy donors, Mol. Ther. Methods Clin. Dev. 14 (2019) 126–133, https://doi.org/10.1016/j.omtm.2019.05.014.

[8] S.J. Aronson, P. Veron, F. Collaud, A. Hubert, V. Delahais, G. Honnet, R.J. de Knegt, N. Junge, U. Baumann, A. Di Giorgio, L. D'Antiga, V.M. Ginocchio, N. Brunetti-Pierri, P. Labrune, U. Beuers, P.J. Bosma, F. Mingozzi, Prevalence and relevance of pre-existing anti-adeno-associated virus immunity in the context of gene therapy for crigler-najjar syndrome, Hum. Gene Ther. 30 (10) (2019) 1297–1305, https://doi.org/10.1089/hum.2019.143.

[9] T. Vandendriessche, L. Thorrez, A. Acosta-Sanchez, I. Petrus, L. Wang, L. Ma, D.E. W. L, Y. Iwasaki, V. Gillijns, J.M. Wilson, D. Collen, M.K. Chuah, Efficacy and safety of adeno-associated viral vectors based on serotype 8 and 9 vs. lentiviral vectors for hemophilia B gene therapy, J. Thromb. Haemostasis 5 (1) (2007) 16–24, https://doi.org/10.1111/j.1538-7836.2006.02220.x.

[10] W.R. Keller, A. Picciano, K. Wilson, J. Xu, H. Khasa, M. Wendeler, Rational downstream development for adeno-associated virus full/empty capsid separation - a streamlined methodology based on high-throughput screening and mechanistic modeling, J. Chromatogr. A 1716 (2024) 464632, https://doi.org/10.1016/j.chroma.2024.464632.

[11] P. Guo, Y. El-Gohary, K. Prasadan, C. Shiota, X. Xiao, J. Wiersch, J. Paredes, S. Tulachan, G.K. Gittes, Rapid and simplified purification of recombinant adeno-associated virus, J. Virol Methods 183 (2) (2012) 139–146, https://doi.org/10.1016/j.jviromet.2012.04.004.

[12] J. El Andari, D. Grimm, Production, processing, and characterization of synthetic AAV gene therapy vectors, Biotechnol. J. 16 (1) (2021) e2000025, https://doi.org/10.1002/biot.202000025.

[13] A.K. Lam, P.L. Mulcrone, D. Frabutt, J. Zhang, M. Chrzanowski, S. Arisa, M. Munoz, X. Li, M. Biswas, D. Markusic, R.W. Herzog, W. Xiao, Comprehensive comparison of AAV purification methods: iodixanol gradient centrifugation vs. Immuno-affinity chromatography, Adv. Cell. Gene Ther. 2023 (2023), https://doi.org/10.1155/2023/2339702.

[14] R.H. Smith, J.R. Levy, R.M. Kotin, A simplified baculovirus-AAV expression vector system coupled with one-step affinity purification yields high-titer rAAV stocks from insect cells, Mol. Ther. 17 (11) (2009) 1888–1896, https://doi.org/10.1038/mt.2009.128.

[15] N. Pulicherla, A. Asokan, Peptide affinity reagents for AAV capsid recognition and purification, Gene Ther. 18 (10) (2011) 1020–1024, https://doi.org/10.1038/gt.2011.46.

[16] J.T. Koerber, J.H. Jang, J.H. Yu, R.S. Kane, D.V. Schaffer, Engineering adeno-associated virus for one-step purification via immobilized metal affinity chromatography, Hum. Gene Ther. 18 (4) (2007) 367–378, https://doi.org/10.1089/hum.2006.139.

[17] M. Florea, F. Nicolaou, S. Pacouret, E.M. Zinn, J. Sanmiguel, E. Andres-Mateos, C. Unzu, A.J. Wagers, L.H. Vandenberghe, High-efficiency purification of divergent AAV serotypes using AAVX affinity chromatography, Mol. Ther. Methods Clin. Dev. 28 (2023) 146–159, https://doi.org/10.1016/j.omtm.2022.12.009.

[18] A.A. Topcu, S. Kilic, E. Ozgur, D. Turkmen, A. Denizli, Inspirations of biomimetic affinity ligands: a review, ACS Omega 7 (37) (2022) 32897–32907, https://doi.org/10.1021/acsomega.2c03530.

[19] G. Fassina, M. Ruvo, G. Palombo, A. Verdoliva, M. Marino, Novel ligands for the affinity-chromatographic purification of antibodies, J. Biochem. Biophys. Methods 49 (1–3) (2001) 481–490, https://doi.org/10.1016/s0165-022x(01)00215-9.

[20] A.M. Eichhoff, K. Borner, B. Albrecht, W. Schafer, N. Baum, F. Haag, J. Korbelin, M. Trepel, I. Braren, D. Grimm, S. Adriouch, F. Koch-Nolte, Nanobody-enhanced targeting of AAV gene therapy vectors, Mol. Ther. Methods Clin. Dev. 15 (2019) 211–220, https://doi.org/10.1016/j.omtm.2019.09.003.

[21] G. Li, M. Zhu, L. Ma, J. Yan, X. Lu, Y. Shen, Y. Wan, Generation of small single domain nanobody binders for sensitive detection of testosterone by electrochemical impedance spectroscopy, ACS Appl. Mater. Interfaces 8 (22) (2016) 13830–13839, https://doi.org/10.1021/acsami.6b04658.

[22] X. Li, P. Qiao, Y. Zhang, G. Liu, M. Zhu, J. Gai, Y. Wan, High performance production process development and scale-up of an anti-TSLP nanobody, Protein Expr. Purif. 218 (2024) 106441, https://doi.org/10.1016/j.pep.2024.106441.

[23] C. Huang, J. Ren, F. Ji, S. Muyldermans, L. Jia, Nanobody-Based high-performance immunosorbent for selective beta 2-microglobulin purification from blood, Acta Biomater. 107 (2020) 232–241, https://doi.org/10.1016/j.actbio.2020.02.028.

[24] M. Sinegubova, I. Vorobiev, A. Klishin, D. Eremin, N. Orlova, N. Orlova, M. Polzikov, Purification process of a recombinant human follicle stimulating hormone biosimilar (primapur((R))) to yield a pharmaceutical product with high batch-to-batch consistency, Pharmaceutics 14 (1) (2022), https://doi.org/10.3390/pharmaceutics14010096.

[25] T.M. Pabst, M. Wendeler, X. Wang, S. Bezemer, P. Hermans, A.K. Hunter, Camelid V(H) H affinity ligands enable separation of closely related biopharmaceuticals, Biotechnol. J. 12 (2) (2017), https://doi.org/10.1002/biot.201600357.

[26] J. Hennicke, A.M. Lastin, D. Reinhart, C. Grunwald-Gruber, F. Altmann, R. Kunert, Glycan profile of CHO derived IgM purified by highly efficient single step affinity chromatography, Anal. Biochem. 539 (2017) 162–166, https://doi.org/10.1016/j.ab.2017.10.020.

[27] J. Fu, J. Li, W. Wang, H. Wu, P. Zhou, Y. Li, Q. He, Z. Tu, One-step orientated immobilization of nanobodies and its application for immunoglobulin purification, J. Chromatogr. A 1603 (2019) 15–22, https://doi.org/10.1016/j.chroma.2019.06.028.

[28] J. Ren, C. Zhang, F. Ji, L. Jia, Characterization and comparison of two peptide-tag specific nanobodies for immunoaffinity chromatography, J. Chromatogr. A 1624 (2020) 461227, https://doi.org/10.1016/j.chroma.2020.461227.

[29] T.A. Stevens, G.P. Tomaleri, M. Hazu, S. Wei, V.N. Nguyen, C. DeKalb, R. M. Voorhees, T. Pleiner, A nanobody-based strategy for rapid and scalable purification of human protein complexes, Nat. Protoc. 19 (1) (2024) 127–158, https://doi.org/10.1038/s41596-023-00904-w.

[30] V. Mashayekhi, E. Schooten, P.M.P. van Bergen En Henegouwen, M.M. Kijanka, S. Oliveira, Nanobody-targeted photodynamic therapy: nanobody production and purification, Methods Mol. Biol. 2451 (2022) 481–493, https://doi.org/10.1007/978-1-0716-2099-1_21.